E≋RS

α′ phase stability in Nd–Li-sialon systems

A.J. Seeber*, Y.-B. Cheng

School of Physics and Materials Engineering, Monash University, Victoria 3800, Australia

Abstract

The formability and stability of the α-sialon (α′) phase was investigated in multi-cation Nd–Li-sialon systems. Four samples were prepared, ranging from a pure Nd-sialon to a pure Li-sialon, with two intermediate samples being prepared with either lithium or neodymium replacing the other α′-stabilising additive by 20 eq.%, as to maintain an equivalent design composition in all samples. After sintering, all samples were subsequently heat treated up to 192 h at 1450 and 1300 °C. While significant quantities of the β′-sialon (β′ phase were found in most samples, the high-lithium Li–Nd-sialon sample was found to be almost pure α′ phase after sintering. Furthermore, the long-term stability of the α′ phase on heat treatment was also found to be superior in both multi-cation samples than in either of the single-α′-stabilising-cation samples. This is thought to be related to improved retention of the lithium in the multi-cation systems, as much of the lithium was found to volatilise during sintering in the neodymium-free sample.
© 2002 Elsevier Science Ltd. All rights reserved.

Keywords: Microstructure-final; Sialons; X-ray methods

1. Introduction

The α-sialon (α′) phase is isostructural with α-Si_3N_4, and can be represented by the general formula $M_{m/v}$ $Si_{12-(m+n)}Al_{(m+n)}O_nN_{16-n}$, where M is an α′-stabilising cation and v is the valency of such a cation. Lithium, calcium, magnesium, yttrium and most rare-earth elements can be used to form the α′ phase.[1] While of interest for it's hardness and strength, of primary concern in recent years has been the stability of the α′ phase to heat treatment.[2–21] The stability of the α′ phase seems to depend on the α′-stabilising cation being used, with α′ phase stability generally being poor where lighter rare-earth stabilising cations such as samarium and neodymium are used.[3–12] While a Li–α-sialon was among the first α′ phases reported[1] it has received limited attention until recently,[21–25] mainly because of problems with densification due to the volatilisation of lithium. Recently, Yu et al.[25] managed to overcome this volatilisation by firing the Li-sialon pellets in a Li-based packing powder, with the resulting materials being high in the α′ phase. The use of multiple α′-stabilising additives has also received some attention,[26–40] with some promising results. In several systems containing poor α′-stabilising cations, an improvement in α′ phase stability has been reported upon the addition of a secondary cation of better α′-stabilising character.[33–40] In this paper, Nd-Li-containing multi-cation α′-sialon systems are investigated.

2. Experimental procedures

Four samples in the Nd–Li-sialon system were produced, based on the α′ compositional formula $m = 0.964$, $n = 1.487$, $k = 0.75$, which placed the composition between the α′- and β′-phase forming regions, near the edge of the α′-phase forming region. In the multi-α′-stabilising-cation samples, lithium was incorporated to replace neodymium on an equivalence basis to conserve the m-value. The design composition is shown projected onto the Nd-α-sialon plane in Fig. 1, and the formulae and equivalent percentage lithium-substitution-for-neodymium in the various samples are shown in Table 1. The starting powders used were Si_3N_4 (H.C. Starck grade LC10, 1.94 wt.% oxygen), AlN (H.C. Starck grade B, 2 wt.% oxygen), Al_2O_3 (Ajax "Labchem"), Nd_2O_3 (Heraeus 99.9%), and Li_2CO_3

---

* Corresponding author.
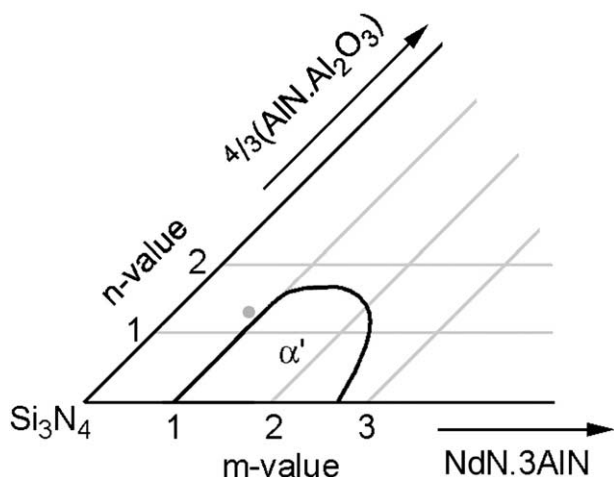*E-mail address:* aaron.seeber@spme.monash.edu.au (A.J. Seeber).

Fig. 1. The design composition as projected onto the Nd α-sialon plane.

Table 1
The formulae and eq.% calcium-substitution-for-samarium for all samples

Sample	Formula	Eq.% Li
Nd10	$Nd_{0.332}Si_{9.854}Al_{2.530}O_{1.535}N_{14.977}$	0
NdLi	$Nd_{0.265}Li_{0.199}Si_{9.854}Al_{2.530}O_{1.535}N_{14.977}$	20
LiNd	$Li_{0.796}Nd_{0.066}Si_{9.854}Al_{2.530}O_{1.535}N_{14.977}$	80
Li10	$Li_{0.995}Si_{9.854}Al_{2.530}O_{1.535}N_{14.977}$	100

(Ajax "Labchem"). Surface oxides on the nitride powders were taken into account when formulating the mixtures, in accordance with the powder specifications provided by the manufacturers. The lithium carbonate powder was air-dried at 200 °C for 48 h then transferred to a desiccator, to remove absorbed water before use. Fifty gram batches of each sample were weighed out, each to within 0.001 g. Powders were milled using Si_3N_4 balls in isopropanol for a period of 24 h, after which the isopropanol was dried off. Powders were then re-mixed by hand for 10 min in an agate mortar and pestle to further homogenise the powder mixture. The powders were uniaxially pressed into pellets ~2.5 cm in diameter and ~1 cm thick, giving pellet weights of approximately 10 g. These pellets were subsequently cold isostatically pressed at 200 MPa.

Samples were first sintered in a graphite resistance furnace under a high purity nitrogen atmosphere. The firing schedule for the Li-free Nd-based sample was as follows: 30 °C/min to 950 °C, hold 30 min; 30 °C/min to 1500 °C, hold 1 h; 5 °C/min to 1820 °C, hold 2 h; then shut-off power and allow to cool to room temperature. The hold at 950 °C was to maintain consistency with previously described samples.[38] A N_2 atmosphere was introduced above 950 °C.

Because of problems with lithium volatilisation,[22] the Li-containing samples were manufactured using a slightly different, two-step process. Li-containing samples were initially pressurelessly sintered in the graphite furnace using the following firing schedule: 30C/min to 1200 °C (for calcination of the Li_2CO_3), hold 30 min; 30 °C/min to 1500 °C, hold 1 h; 5 °C/min to 1750 °C, hold 1 h, then shut-off power and allow to cool to room temperature. A N_2 atmosphere was introduced above 1200 °C. Samples were then hot pressed using a graphite die under a high purity nitrogen atmosphere at a temperature of 1750 °C for 1 h, using a pressure of 20 MPa. Pressure was initially applied at 1500 °C and slowly increased to 20 MPa at 1750 °C. Again, heating rates were 30 °C/min up to 1500 °C and 5 °C/min above this temperature.

Heat treatment of samples took place in an alumina tube furnace, again using a high purity nitrogen atmosphere. Heating rates used were 5 °C/min up to 800 °C, 3 °C/min above this temperature, with equivalent cooling rates. The sintered samples were heat treated at 1300 and 1450 °C, up to 192 h (8 days) at each temperature.

XRD analysis was performed with a Rigaku Geigerflex diffractometer using Ni-filtered Cu K_α radiation. The ratio of α' to β' was determined by the method of XRD peak mean-normalised-intensity of Gazzara and Messier[41] as developed by Li and O'Connor.[42] A number of peaks were used for both the α' and β' phases, to eliminate texture effects in the hot-pressed samples. The normalising factors were calculated using the program "Volfract".[43]

The ^{7}Li-NMR analysis was performed using a 7.05T Bruker AS2000 Spectrometer, operating at 116.642 MHz. Samples were weighed and loaded into a 7 mm rotor and static spectra were obtained using single $\pi/4$ pulses and a sweep-width of 50 kHz. The resultant spectra were curve-fitted using a basic Gaussian–Lorentzian lineshape to obtain the relative areas under each curve, and then normalised relative to the number of pulses (720 for the standard and 1000 for the sample) and amount of sample.

Micrographs were obtained using a Jeol JSM 840A operating at 20 kV, prior to which the samples were carbon-coated.

3. Results

3.1. Phase stability during sintering

In order to briefly investigate phase formation on the way to sintering temperature, pellets of each of the samples were fired at 1200 and 1500 °C and held for 10 min, and subsequently investigated via X-ray diffraction (XRD). These temperatures are significant to these systems, being the temperature where Li_2CO_3 is expected to decompose to Li_2O and CO_2, (1200 °C), and the approximate temperature at which α' phase formation is thought

to begin in both the Nd–Si–Al–O–N and Li–Si–Al–O–N systems.[14] XRD results from both of these firings are presented in Table 2. At 1200 °C, it can be seen that reactions between the starting powders have been minimal. The only new phase found is a Li–Nd-apatite phase in both of the multi-cation samples. Apart from this, only α- and β-Si_3N_4, AlN and Nd_2O_3 are observed through significant intensities in the XRD spectra. Note that the lithium carbonate is expected to have decomposed to lithia at 1200 °C, but the absence of either lithium carbonate or lithia in the XRD spectra may be explained in terms of the lower diffracted intensities expected from such relatively light phases, present in such small quantities. Also, a Li–Al-containing glass might be formed, as might be reasoned from the lack of Al_2O_3 peaks in all Li-containing samples. Note also that the Nd_2O_3 phase is a strongly diffracting one, hence producing abnormally large reflections in these spectra compared with the other phases present.

At 1500 °C, the apatite phases in the Nd–Li-containing samples have melted, and traces of the α′ phase are observed in these samples. No sialon phases are yet observed in either of the single-α′-stabilising-additive samples. While the α′ phase has previously been reported in Li-sialon systems at lower temperatures,[13,25] the hold times at temperature in these cases were appreciably longer than the 10 min used here. Furthermore, while the AlN phase was still observed in all samples, it was found in smaller quantities in both the multi-cation samples, as would be expected given that α′ phase formation is observed. A β-LiSiON phase was found in the

high-Li Li10 and LiNd samples, with greater quantities of this phase being found in the Li10 sample. Presumably, both α′ phase formation and the lower quantities of lithium found in the LiNd sample have resulted in a reduction of the amount of the β-LiSiON phase produced in this sample. The $NdAlO_3$ phase was observed to form in the pure-Nd Nd10 sample at 1500 °C, but this is the only reaction observed to have occurred at this stage in this sample. It was also noted that some β-sialon was found in the high-Nd NdLi sample, though not in any of the other samples. This may be related to a reduction in grain boundary glass viscosity due to the inclusion of lithium in the NdLi sample, and also to the suppression of $NdAlO_3$ formation, as the precipitation of this phase would hinder glass formation in the Nd10 sample.

3.2. Samples in the as-fired state

All other XRD results (for samples both in the as-fired state and also after subsequent heat treatments) are presented in Table 3. Both the α′ and β′ phases were found in all samples, along with an AlN polytypoid phase, although only a trace of the β′ phase was found in the high-Li LiNd sample, with β′ content being appreciably higher in all other samples. The 21R AlN polytypoid phase was found in the Nd-rich Nd10 and NdLi samples, 12H was found in the Li-rich LiNd sample and 8H was found in the Nd-free Li10 sample—in other words, the Si–O content of the AlN polytypoid phases is observed to increase in the higher lithium-content samples. Other than these phases, appreciable quantities of a Nd–melilite (M'_{ss}) phase were found in the Li-free Nd10 sample, and also of Nd–N–wollastonite in the Nd-rich NdLi sample. A trace of the Nd-sialon U-phase was found in the Li-rich LiNd sample, and no additional phases were observed in the Nd-free Li10 sample.

The amount of α′ phase present in the high-Li samples is worth further consideration. With lithium being a monovalent α′-stabilising additive, significant quantities of this α′-stabilising cation were added relative to trivalent neodymium. Consequently, the Li10 sample should contain no β′ phase on the basis of x-value, as equivalent design places the x-value of the pure-Li Li10 sample equal to the m-value, i.e. at 0.964. However, α′ phase formability in this sample is reasonably low, indicating that lithium volatility may be a problem. NMR analysis of lithium content in the Li10 sample was performed relative to a standard solution of known lithium content, which indicated that ∼80% of the designed lithium has left the system. This explains the high β′ content in the Li10 sample. Therefore, the amount of lithium that remains in the system places the α′-stabilising cation content for the Li10 sample lower than the designed x-value in the trivalent α′-stabilising

Table 2
XRD data for the samples as fired at 1200 and 1500 °C

Sample		1200 °C	1500 °C
Nd10	α/β	93/7	85/15
	Other phases	AlN (M)	AlN (M)
		Nd_2O_3 (S)	A (S)
		Al_2O_3 (VW)	
NdLi	α/β	88/12	85/15*
	Other phases	AlN (MW)	AlN (MW)
		Ap[a] (W)	
		Nd_2O_3 (MW)	
LiNd	α/β	89/11	88/12**
	Other phases	AlN (M)	AlN (MW)
		Ap (W)	L[b] (W)
		Nd_2O_3 (W)	
Li10	α/β	89/11	92/8
	Other phases	AlN (M)	AlN (M)
			L (MW)

α/β is given in wt.%, and represents Si_3N_4 phases, not sialon phases.
[a] Ap = Neodymium–lithium-apatite: $Nd_9Li(SiO_4)_6O_2$.
[b] L = β-LiSiON.
* Some α′ present.
** Some α′ and β′ present.

Table 3
XRD data for the samples as-fired, and after heat-treatment for various times (α'/β' is given in wt.%)

Sample		As fired	24 h 1450 °C	48 h 1450 °C	96 h 1450 °C	192 h 1450 °C	24 h 1300 °C	96 h 1300 °C	192 h 1300 °C
Nd10	α'/β'	64/36	35/65	9/91	0/100	0/100	61/39	51/49	45/55
	Other phases	21R (W)	21R (W)	21R (W)	21R (W)	21R (MW)	21R (W)	21R (W)	21R (VW)
		M'_{ss} (MW)	M'_{ss} (MS)	M'_{ss} (S)	M'_{ss} (S)	M'_{ss} (S)	M'_{ss} (VW)	M'_{ss} (VW)	A (M)
							A[a] (MW)	A (M)	
NdLi	α'/β'	71/29	67/33	62/38	59/41	61/39	65/35	64/36	64/36
	Other phases	21R (W)	21R (W)	21R (W)	21R (W)	21R (W)	21R (W)	21R (W)	21R (W)
		W[b] (MW)	A (MW)	A (W)	A (W)	A (W)	A (MW)	A (MW)	A (MW)
				M'_{ss} (MW)	M'_{ss} (W)	M'_{ss} (MW)			
LiNd	α'/β'	99/1	99/1	99/1	99/1	99/1	99/1	99/1	99/1
	Other phases	12H (VW)	12H (VW)	12H (VW)	12H (VW)	12H (VW)	12H (VW)	12H (VW)	12H (VW)
		U[c] (VW)	U (W)	U (W)	U (W)	U (W)	U (W)	U (VW)	U (W)
Li10	α'/β'	82/18	68/32	60/40	50/50	7/93	77/23	70/30	43/57
	Other phases	8H (VW)	8H (VW)	8H (W)	8H (W)	8H (W)	8H (VW)	8H (VW)	8H (W)

[a] A = Neodymium aluminate: $NdAlO_3$.
[b] W = Neodymium–nitrogen–wollastonite: $NdSiO_2N$.
[c] U = Nd-Sialon U-phase: $Nd_3Si_3Al_3O_{12}N_2$.

cation samples in this series, that is, at $x = 0.2$ in the Li-based sample as opposed to $x = 0.321$ in the Nd-based sample. Despite this, the α' phase content in the Li10 sample is comparable with that found in the high-neodymium samples, suggesting that most of the remaining lithium is incorporated into the α' phase, and that little glass remains. It should be noted that a lower minimum solubility ($x = 0.25$) has been recorded for lithium to form the α' phase[22] as opposed to neodymium, where the minimum solubility is thought to be closer to $x = 0.3$. Such a lower minimum solubility would also increase the amount of Li-α' phase found in this sample on the basis of x-value relative to a Nd-stabilised α' phase. The NMR spectra used for these analyses are presented in Fig. 2.

In comparison with the Nd-free Li10 sample, the Li-rich LiNd sample is almost pure α' phase, with only a small quantity of β' being found. The amount of neodymium used is far too small to produce such an increase in the quantity of α' phase by itself, given the poor α'-forming character of the Nd–Si–Al–O–N system. Therefore, this marked improvement in α' formability indicates that the incorporation of a small amount of a rare earth oxide into a Li-sialon system may help reduce the volatility of the lithium. This is a particularly significant result for this sample, given that the small quantity of neodymium present in this sample must be all that is required to retain adequate quantities of the lithium.

The lack of additional grain boundary phases in the Nd-free Li10 sample is readily understood, given the volatility of lithium. Likewise, since the M'_{ss} phase has previously been found to form in the Nd–Si–Al–O–N system during sintering and be residual at 1850 °C,[44] the presence of this phase in the Li-free Nd10 sample is expected. However, the M'_{ss} phase is not observed on sintering in either of the two multi-cation samples, with N–wollastonite being found in the NdLi sample and the U-phase being found in the LiNd sample. Therefore, the incorporation of even a small amount of lithium is found to retard Nd-M'_{ss} phase formation, a factor which would lead to greater α' phase formability and improved sinterability, given the highly refractory nature of the Nd-M'_{ss} phase. It is assumed that these Nd-based phases in the Nd–Li-containing samples have formed during cooling, where the lower viscosity of the grain boundary glass due to the presence of lithium has allowed these phases to form. Both of these phases have previously been observed as devitrification products in α'-containing Nd–Si–Al–O–N systems during heat treatment at 1150 °C.[6]
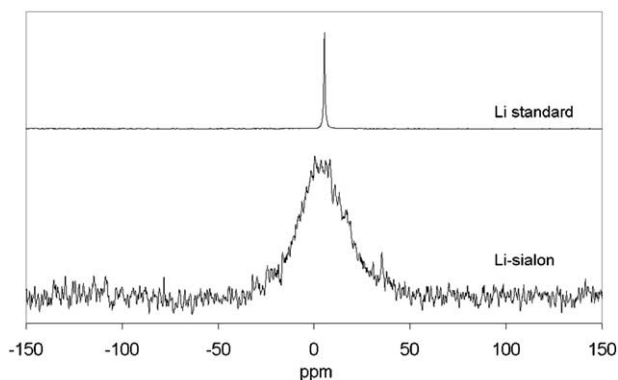

Fig. 2. Static ^7Li NMR spectra used to quantify the amount of Li present in the as-fired Li-sialon sample. Spectra were curve-fitted using standard Gaussian–Lorentzian line-shapes.
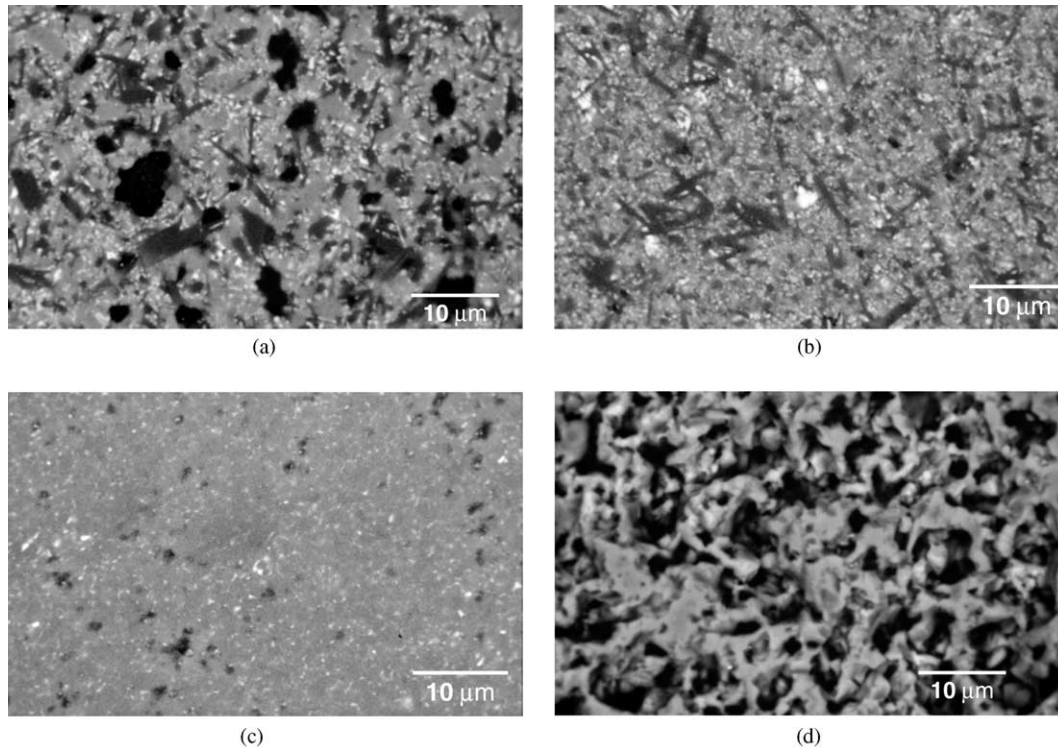
Fig. 3. The microstructures of all samples in the as-fired state: (a) Nd10 (b) NdLi; (c) LiNd; (d) Li10.

Micrographs of the as-fired samples are shown in Fig. 3. As the Li-free Nd10 sample was not hot-pressed, and M'_{ss} was found to be residual in the sample on sintering, the high porosity in this sample is understandable. Likewise, the low density of the hot-pressed Li10 sample is attributable to lithium volatilisation, which has reduced the amount of lithium available for forming a liquid phase during sintering. The higher density of the two multi-cation samples is further evidence of the retention of lithium when used in conjunction with neodymium as another sintering additive.

Apart from density, Fig. 3(b) shows the α' phase grain size in the high-Nd NdLi sample to be considerably smaller than that found in the Li-free Nd10 sample, an observation that also seems to hold for the high-Li LiNd sample. This may be due to the combination of a low α'-forming temperature for both neodymium and lithium[14] with a substantial reduction in glass viscosity due to the presence of lithium allowing greater mobility, enhancing low temperature α' phase nucleation, which would lead to a reduction in α' grain size. It was noted in Section 3.1 that the α' phase is observable in both Nd–Li-containing samples after 10 min at 1500 °C, at which point no sialon formation had yet been observed in either of the single-α'-stabilising-additive samples.

3.3. The samples after heat treatment at 1450 °C

Heat treatment at 1450 °C has resulted in $\alpha' \rightarrow \beta'$ transformation in most samples. The ratio of $\beta':(\alpha' + \beta')$

in all samples before and after the 1450 °C heat treatment is shown in Fig. 4. The α' phase in the Nd10 sample was found to be extremely unstable, and has completely transformed to β' after 96 h heat treatment at 1450 °C. Likewise, the α' phase in the Nd-free Li10 sample is also quite unstable, and has almost disappeared after 192 h heat treatment at 1450 °C. However, the α' phase in both of the multi-cation samples is significantly more stable than in either of the single-additive samples. No $\alpha' \rightarrow \beta'$ transformation is observed in the high-Li LiNd sample, and the transformation is only observed in the initial stages of heat treatment in the high-Nd NdLi sample. The amount of β' phase in the Nd-free Li10 sample has overtaken that in the NdLi sample after 48 h of heat treatment, and continues at a
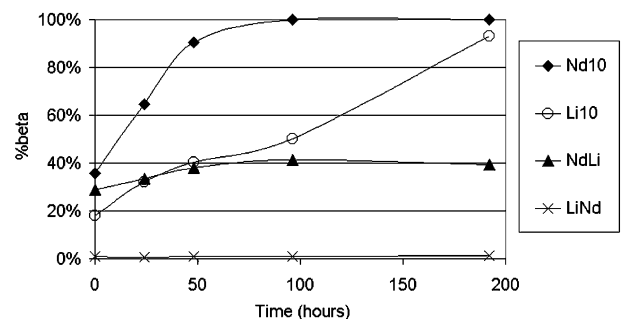

Fig. 4. The percentage of the β' phase in all samples prior to and after heat treatments at 1450 °C.% β' is taken as a function of α' and β' only.

fairly constant rate, whereas no significant differences in β' content are observed in the high-Nd NdLi sample after this time.

As shown in Table 3, no additional products are found in the Li10 sample as heat treatment progresses. This helps to explain the sustained rate of $\alpha' \rightarrow \beta'$ transformation observed in this sample, as the Li-rich glass which would be expected to form upon α' phase decomposition does not appear to be devitrified. The M'_{ss} phase in the Nd10 sample grows markedly as the α' phase transforms to β', and no changes in the phases present are observed in the sample after 96 h heat treatment at 1450 °C, at which point the α' phase has disappeared. It is suggested that the M'_{ss} phase is a by-product of the $\alpha' \rightarrow \beta'$ transformation at 1450 °C, in which the extra neodymium and other species in the α' phase are incorporated in the M'_{ss} after α' transforms to β'. The amount of U-phase found in the high-Li LiNd sample does not appear to change significantly, which is unsurprising given that no other transformations are observed in this sample. The lack of new phases in the LiNd sample may be also due to the low melting point of Li-based grain boundary phases, which prevents crystallisation of Li-based phases at 1450 °C, but since Fig. 3(c) showed the LiNd sample to consist largely of the α' phase, any additional phases would in any case be quite minor. The only sample to produce a new phase on heat treatment is the NdLi sample, in which the N–wollastonite is observed to disappear in the initial stages of heat treatment. After the first 24 h of heat treatment at 1450 °C, $NdAlO_3$ is the only new phase present, and M'_{ss} does not appear until after 48 h heat treatment. After this stage, M'_{ss} appears to be the dominant grain boundary phase in the NdLi sample. Either lithium has increased the thermal stability of the $NdAlO_3$ phase, or this $NdAlO_3$ is formed on cooling. It seems unlikely that the monovalent lithium cation is soluble within the $NdAlO_3$ phase, so it appears that the reduced viscosity of the Li-containing residual glass has enabled $NdAlO_3$ devitrification during cooling. It was noted in Section 3.2 that the incorporation of lithium had retarded Nd-M'_{ss} formation on sintering, so this hindrance may also be extended to slowing the formation of the M'_{ss} phase during heat treatment. As Nd levels increase in the grain boundaries, the hindrance is slowly overcome, and more Nd-M'_{ss} forms. Another possible explanation is that given the expected high solubility of lithium within the α' phase, a greater quantity of neodymium may be present in the glass in the NdLi sample as compared with the pure-Nd Nd10 sample. No $NdAlO_3$ phase was formed during the 1450 °C heat treatment in the Nd10 sample, as the M'_{ss} phase was already present during sintering.

Micrographs of selected samples after heat-treatment at 1450 °C are shown in Fig. 5. Since no changes were observable in the Nd-free Li10 sample due to a lack of compositional contrast, this sample is not presented. Large quantities of M'_{ss} are visible in the pure-Nd Nd10 sample in Fig. 5(a) and (b), a sample which was observed to undergo complete $\alpha' \rightarrow \beta'$ phase transformation. The large M'_{ss} grains found in this sample appear to be segregated in the microstructure, as has been described elsewhere.[40] As a result, β'-rich regions and M'_{ss}-rich regions can easily be distinguished. M'_{ss} phase segregation is even more prominent in the Li-containing NdLi sample, as shown in Fig. 5(c) through (e). This may be due to a decrease in grain boundary liquid viscosity owing to the incorporation of lithium cations. This would allow for more rapid mass transfer and therefore greater growth of the M'_{ss} grains.

3.4. The samples after heat treatment at 1300 °C

Heat treatment at 1300 °C has resulted in $\alpha' \rightarrow \beta'$ transformation in most samples, though not to the same extent as observed during the 1450 °C heat treatment. The ratio of $\beta':(\alpha' + \beta')$ in all samples before and after the 1300 °C heat treatment is shown in Fig. 6. Continued $\alpha' \rightarrow \beta'$ phase transformation is observed in both of the single-α'-stabilising cation samples, little transformation is observed in the Nd-rich NdLi sample, and no transformation is observable in the high-Li LiNd sample. The low stability of the α' phase in the pure-Li Li10 sample stands out in particular. After 192 h heat treatment at 1300C, the amount of β' phase in the Li10 sample exceeds that found in the pure-Nd Nd10 sample, despite the fact that considerably less β' phase is found in the Li10 sample after the initial sintering.

Few devitrification products are observable in these samples after a 1300 °C heat treatment. As was found during the 1450 °C heat treatment, no additional phases are observed to form in the pure-Li Li10 sample. Likewise similar with the results from the 1450 °C heat treatment, the U-phase is found in the high-Li LiNd sample, and in quantities comparable to those found prior to heat treatment. Given that no $\alpha' \rightarrow \beta'$ phase transformation was observable in the LiNd sample, the lack of grain boundary phase development is understandable. Also, the N–wollastonite phase found on sintering in the high-Nd NdLi sample disappears on heat treatment, but the $NdAlO_3$ phase is the only devitrification product found, with no M'_{ss} phase being formed in this sample at 1300 °C. The only difference is found in the Nd10 sample, which produces a $NdAlO_3$ phase on heat treatment. The M'_{ss} phase found in the as-fired state in this sample dwindles to a trace during the initial 24 h of heat treatment at 1300 °C, disappearing altogether after 192 h at 1300 °C. This suggests that the M'_{ss} is thermodynamically unstable to $NdAlO_3$ at 1300 °C.

Micrographs of selected samples after heat-treatment at 1300 °C are shown in Fig. 7. Again, as no change was observable in the Nd-free Li10 sample due to a lack of compositional contrast, this sample is not presented. Smaller quantities of the grain boundary phases are seen in these samples after heat treatment at 1300 °C as compared with a 1450 °C heat treatment. Regarding the pure-Nd Nd10 sample, as shown in Fig. 7(a), the NdAlO$_3$ grains developed at 1300 °C are seen to be finer and more evenly distributed than the M$'_{ss}$ grains developed in this sample at 1450 °C, which was shown in Fig. 5(a) and (b). The phase segregation found in the high-Nd NdLi sample after heat treatment at 1450 °C is not repeated in the 1300 °C heat treatment, during which the M$'_{ss}$ phase is not produced.
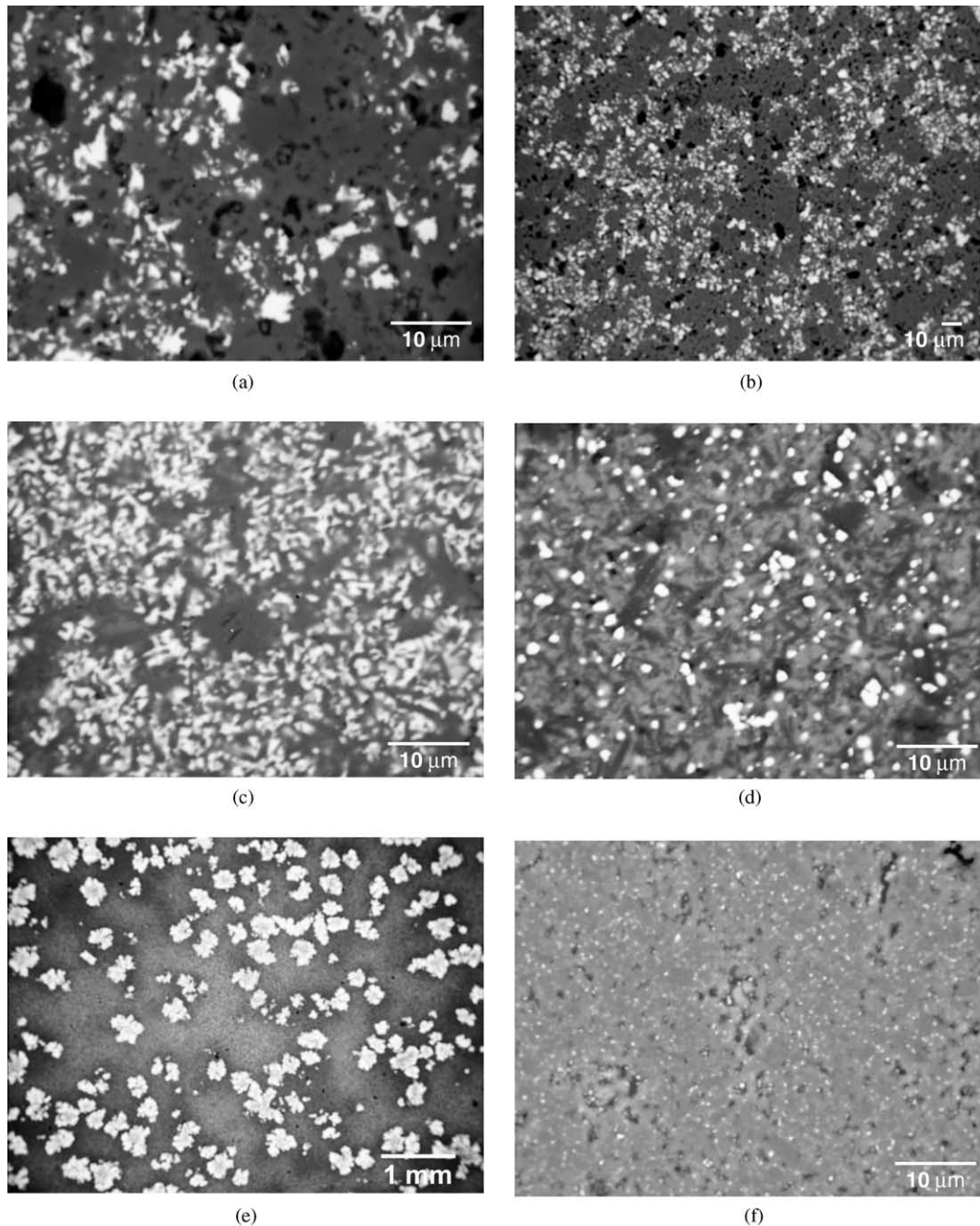

Fig. 5. The microstructures of all Nd-containing samples after 192 h heat treatment at 1450 °C: (a) Nd10 high-magnification; (b) Nd10 low-magnification; (c) NdLi high-magnification, M$'_{ss}$-rich region; (d) NdLi high-magnification, M$'_{ss}$-poor region; (e) NdLi low-magnification; (f) LiNd.
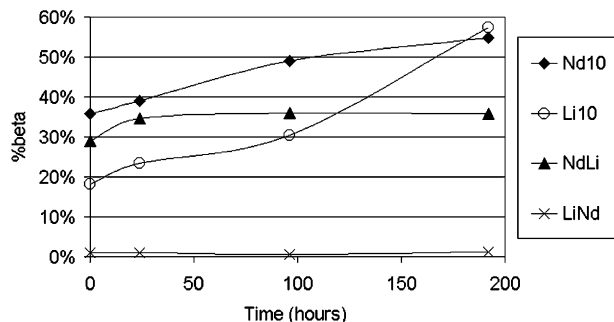
Fig. 6. The percentage of the β' phase in all samples prior to and after heat treatments at 1300 °C.% β' is taken as a function of α' and β' only.

4. Discussion

The behaviour of the α' phase in the pure-Li Li10 sample is worth further consideration. Firstly, because of the loss of most of the lithium to volatilisation on firing, the α' phase in this sample is thermodynamically unstable. The α' phase region is expected to be significantly larger at the sintering temperature (1750 °C/ 1820 °C) than at the heat treatment temperatures (1300– 1450 °C), which means that on heat treatment the sample is placed well outside the single-α' phase region and well inside the mixed α'/β' phase region. Secondly, the high rate of transformation even at 1300 °C may be related to the low viscosity of the liquid phase in the Li-containing sample, which would allow easier mass transfer than the liquid phases found in the other systems in this series. While little liquid is expected to be present prior to heat treatment, it still appears to be sufficient to facilitate the transformation, and given the lack of devitrification products a Li-rich glass would be expected to develop upon continued heat treatment. At 1300 °C, heat treatment of all Nd-containing samples has resulted in an oxygen-rich devitrification product, which would be expected to reduce the viscosity of the remaining grain boundary glass, whereas no such devitrification product is observed to form in the pure-Li Li10 sample. This would serve to further exacerbate the problem of α' phase transformability in this sample.

It can be seen from these results that the stability of the α' phase in both multi-cation samples is improved relative to each of those samples where only one α'-stabilising additive has been used. Firstly, though the high-Nd NdLi sample contains greater quantities of the β' phase than the pure-Li Li10 sample on sintering, the α' phase in the NdLi sample still appears to be more stable
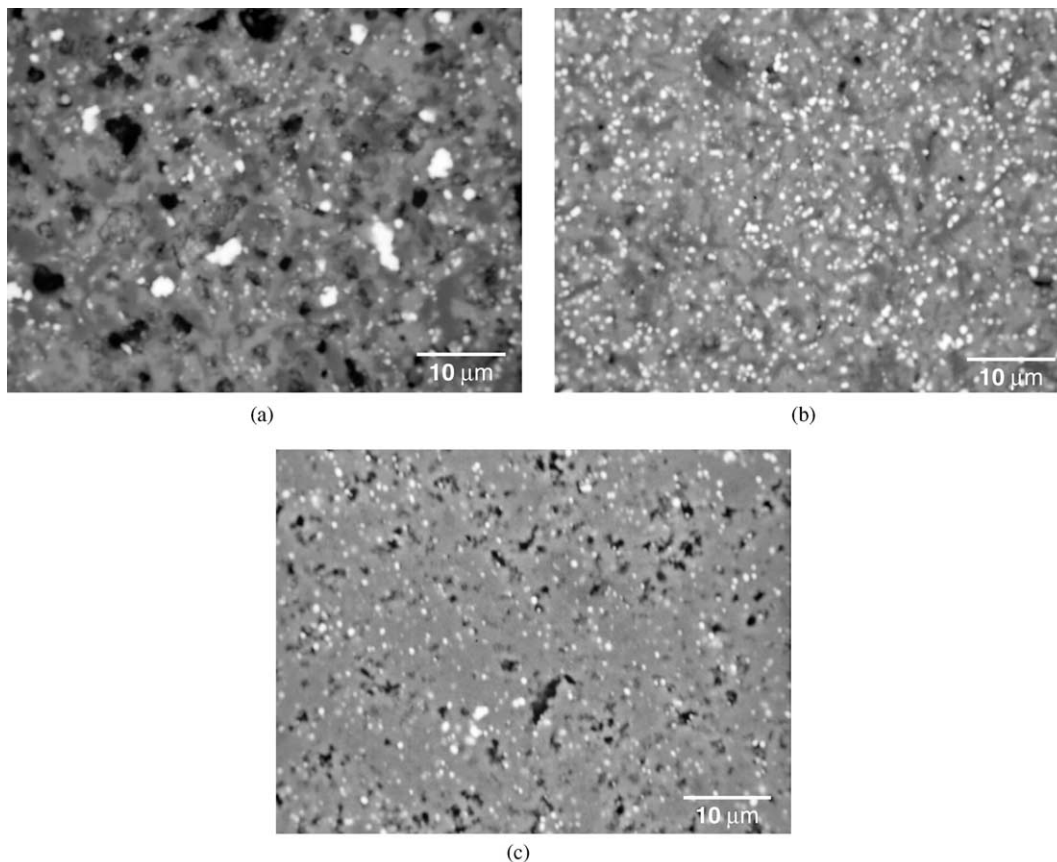

(a)

(b)

(c)

Fig. 7. The microstructures of all Nd-containing samples after 192 h heat treatment at 1300 °C: (a) Nd10 (b) NdLi; (c) LiNd.

on heat treatment than that found in the Li10 sample. This can be explained in terms of the relative diffusivity through the grain boundary liquid on heat treatment—the pure-Li Li10 sample would be expected to have a considerably lower viscosity than that in the NdLi sample, thus enhancing mass transport. Secondly, the high-Li LiNd sample contains considerably greater quantities of the α′ phase than any of the other samples, and the α′ phase also seems to be quite stable on heat treatment. It was noted earlier that most of the lithium in the pure-Li Li10 sample appears to have been volatilised during sintering. Volatilisation of lithium has long been recognised as a problem for α′ phase formation,[45] and Yu et al.[25] recently found that lithium volatility could be reduced by using a Li-containing packing powder. However, the present results show that lithium volatilisation can also be reduced by using lithium in conjunction with a second α′-stabilising additive. In the high-Li LiNd sample, the incorporation of a small amount of neodymium has significantly reduced the volatility of lithium on sintering, allowing more of it to be retained for α′ phase formation. This reduced volatilisation is due to two reasons: the formation of an apatite-based phase at 1200 °C, and the early formation of the α′ phase at 1500 °C. Furthermore, early formation of the α′ phase is indicative of an increase in the size of the α′ phase region in the multi-cation samples at these lower temperatures. This would also tend to improve the stability of the α′ phase in these samples. An improvement in α′ phase formability has been observed before in Nd–Li-sialon ceramics when compared with their single-α′-stabilising-cation counterparts.[26] However, the observation in this study is still significant, as only a small degree of neodymium-for-lithium substitution was found to be necessary in order to produce significant quantities of the α′ phase. The work by Redington et al.[26] concentrated on low Li:Nd equivalence ratios of 40:60, and 14:86 eq.%, as opposed to the 80:20 eq.% design ratio in the high-Li LiNd sample in this study.

5. Conclusions

1. The use of lithium in conjunction with neodymium as a secondary α′-phase forming additive has improved α′ phase formability relative to both single cation systems. This is seen through the formation of the α′ phase after 10 min at 1500 °C, and the formation of higher quantities of the α′ phase after sintering.

2. Volatilisation of lithium during sintering can be reduced through the incorporation of a secondary α′-stabilising additive, such as neodymium.

3. Furthermore, the stability of such a multi-cation α′ phase to heat treatment is improved relative to both single cation systems, due to both an increase in the size of the α′-phase forming region and an increase in the overall amount of the α′ phase present.

References

1. Hampshire, S., Park, H. K., Thompson, D. P. and Jack, K. H., α′-sialon ceramics. *Nature*, 1978, **274**, 880–882.

2. Mandal, H., Thompson, D. P. and Ekstrom, T., Reversible α↔β sialon transformation in heat-treated sialon ceramics. *J. Eur. Ceram. Soc.*, 1993, **12**, 421–429.

3. Cheng, Y.-B. and Thompson, D. P., Preparation and grain boundary devitrification of samarium α-sialon ceramics. *J. Eur. Ceram. Soc.*, 1994, **14**, 13–21.

4. Mandal, H., Camuscu, N. and Thompson, D. P., Comparison of the effectiveness of rare-earth sintering additives on the high-temperature stability of α-sialon ceramics. *J. Mat. Sci.*, 1995, **30**, 5901–5909.

5. Zhao, R. and Cheng, Y.-B., Phase transformations in Sm (α + β)-sialon ceramics during post-sintering heat treatments. *J. Eur. Ceram. Soc.*, 1995, **15**, 1221–1228.

6. Shen, Z., Ekstrom, T. and Nygren, M., Reactions occurring in post heat treated α/β sialons: on the thermal stability of α-sialon. *J. Eur. Ceram. Soc.*, 1996, **16**, 873–883.

7. Shen, Z., Ekstrom, T. and Nygren, M., Homogeneity region and thermal stability of neodymium-doped α-sialon ceramics. *J. Am. Ceram. Soc.*, 1996, **79**, 721–732.

8. Zhao, R. and Cheng, Y.-B., Decomposition of Sm α-sialon phases during post-sintering heat treatment. *J. Eur. Ceram. Soc.*, 1996, **16**, 1001–1008.

9. Mandal, H. and Thompson, D. P., Thermal stability of rare-earth densified α-sialon ceramics. *Key Eng. Mat.*, 1997, **132–136**, 990–993.

10. Camuscu, N., Thompson, D. P. and Mandal, H., Effect of starting composition, type of rare earth sintering additive and amount of liquid phase on α↔β sialon transformation. *J. Eur. Ceram. Soc.*, 1997, **17**, 599–613.

11. Mitomo, M. and Ishida, A., Stability of α-sialons in low temperature annealing. *J. Eur. Ceram. Soc.*, 1999, **19**, 7–15.

12. Liu, Q., Gao, L., Yan, D. S. and Thompson, D. P., Thermal stability and mechanical performance of multiply heat-treated α-sialon ceramics densified with rare-earth oxides. *J. Mat. Sci.*, 2000, **35**, 2229–2233.

13. Menon, M. and Chen, I. W., Reaction densification of α′-sialon: I, Wetting behaviour and acid-base reactions. *J. Am. Ceram. Soc.*, 1995, **78**, 545–552.

14. Menon, M. and Chen, I. W., Reaction densification of α′-sialon: II, Densification behaviour. *J. Am. Ceram. Soc.*, 1995, **78**, 553–559.

15. Sun, W. Y., Wang, P. L. and Yan, D. S., Phase transformation in Ln-(α + β)-sialon ceramics by heat treatment. *Mat. Lett.*, 1996, **26**, 9–16.

16. Ekstrom, T., Falk, L. and Shen, Z. J., Duplex α,β-sialon ceramics stabilised by dysprosium and samarium. *J. Am. Ceram. Soc.*, 1997, **80**, 301–312.

17. Swenser, S. P., Pereloma, E. V. and Cheng, Y.-B., Nano-inclusions associated with b-sialon grains in α–β sialon materials. *Key Eng. Mat.*, 1997, **132–136**, 1014–1017.

18. Zhao, R., Swenser, S. P. and Cheng, Y.-B., Formation of AlN-polytypoid phases during α-sialon decomposition. *J. Am. Ceram. Soc.*, 1997, **80**, 2459–2463.

19. Hewett, C. L., Cheng, Y.-B., Muddle, B. C. and Trigg, M. B., Thermal stability of calcium α-sialon ceramics. *J. Eur. Ceram. Soc.*, 1998, **18**, 417–427.

20. Mandal, H. and Thompson, D. P., a→b sialon transformation in calcium-containing α-sialon ceramics. *J. Eur. Ceram. Soc.*, 1999, **19**, 543–552.

21. Yu, Z., Thompson, D. P. and Bhatti, A. R., Transformation and thermal stability of Li-α-sialon ceramics. *J. Eur. Ceram. Soc.*, 2000, **20**, 1815–1828.

22. Kuang, S. F., Huang, Z. K., Sun, W. Y. and Yen, T. S., Phase relationships in the Li₂O–Si₃N₄-AlN system and the formation of lithium-α′-sialon. *J. Mat. Sci. Lett.*, 1990, **9**, 72–74.

23. Kempgens, P., Harris, R. K., Yu, Z. B. and Thompson, D. P., Structural characterization of Li alpha-sialon ceramics by high-resolution Al-27 and Si-29 NMR spectroscopy. *J. Mater. Chem.*, 2001, **11**, 2507–2512.

24. Yu, Z. B., Thompson, D. P. and Bhatti, A. R., In situ growth of elongated alpha-sialon grains in Li-alpha-sialon ceramics. *J. Eur. Ceram. Soc.*, 2001, **21**, 2423–2434.

25. Yu, Z. B., Thompson, D. P. and Bhatti, A. R., Preparation of single phase lithium α-sialons. *Brit. Ceram. Trans.*, 1998, **97**, 41–47.

26. Redington, M. and Hampshire, S., Multi-cation α-sialons. *Br. Ceram. Proc.*, 1992, **49**, 175–190.

27. Huang, Z. K., Jiang, Y. Z. and Tien, T. Y., Formation of α-sialons with dual modifying cations (Li + Y and Ca + Y). *J. Mat. Sci. Lett.*, 1997, **16**, 747–751.

28. Mandal, H., Oberacker, R., Hoffmann, M. J. and Thompson, D. P., α-sialon ceramics densified with mixed oxide sintering additives. 2000.

29. Wang, P. L., Li, Y. W. and Yan, D. S., Effect of amount and atomic ratio of dual modifiers Ca and Mg on phase formation and mechanical properties of Ca,Mg-alpha-Sialons. *J. Mat. Sci.*, 2000, **35**, 1585–1588.

30. Mandal, H., Hoffmann, M. J., Thompson, D. P. and Jack, K. H., α↔β sialon transformation in multi-cation doped α-sialon ceramics, In 9th Cimtec World Ceramics Congress and Forum on New Materials, ed. P. Vincenzini. 1999, pp. 137–144.

31. Zhang, C., Sun, W. Y. and Yan, D. S., Characteristic of (Dy + Sm)-sialon ceramics. *Key Eng. Mat.*, 1999, **161–163**, 239–242.

32. Wang, P. L., Zhang, C., Sun, W. Y. and Yan, D. S., Formation behaviour of multi-cation α-sialons containing calcium and magnesium. *Mat. Lett.*, 1999, **38**, 178–185.

33. Hwang, C. J., Susnitszky, D. W. and Beaman, D. R., Preparation of multication α-sialon containing strontium. *J. Am. Ceram. Soc.*, 1995, **78**, 588–592.

34. Seeber, A. J. and Cheng, Y.-B., High temperature stability of α-sialons containing mixed cations. *Key Eng. Mat.*, 1997, **132–136**, 980–983.

35. Zhang, C., Sun, W. Y. and Yan, D. S., Optimizing mechanical properties and thermal stability of Ln-α-β-sialon by using duplex Ln elements (Dy and Sm). *J. Eur. Ceram. Soc.*, 1999, **19**, 33–39.

36. Mandal, H. and Hoffmann, M. J., Preparation of multiple-cation α-sialon ceramics containing lanthanum. *J. Am. Ceram. Soc.*, 1999, **82**, 229–232.

37. Seeber, A. J. and Cheng, Y. -B., The stabilization of Nd-sialons through calcia additions, In Proceedings of the 1st China International Conference on High-Performance Ceramics, ed. D. S. Yan. Tsinghua Uni Press, 1999, pp. 250–253.

38. Seeber, A. J., Phase Stability in Multi-cation α-Sialon Systems. PhD thesis, Monash University, Melbourne, 2000.

39. Li, Y. W., Wang, P. L., Chen, W. W., Cheng, Y. B. and Yan, D. S., Formation behavior, microstructure and mechanical properties of multi-cation alpha-sialons containing calcium and neodymium. *J. Eur. Ceram. Soc.*, 2001, **21**, 1273–1278.

40. Seeber, A. J., Cheng, Y. -B. and Harrowfield, I. Phase and microstructural evolution during the heat treatment of Sm–Ca-α-sialon ceramics *J. Eur. Ceram. Soc.*, 2002, **22**, 1609–1620.

41. Gazzara, C. P. and Messier, D. R., Determination of phase content of Si₃N₄ by X-ray diffraction analysis. *Ceram. Bull.*, 1977, **56**, 777–780.

42. Li, D. Y., O'Connor, B. H., Chen, Q. T. and Zadnik, M. G., Quantitative powder X-ray diffractometry phase analysis of silicon nitride materials by a multiline, mean-normalized-intensity method. *J. Am. Ceram. Soc.*, 1994, **77**, 2195–2198.

43. Payne, J., *Volfract, 1.4*. MIT, Houghton, MI, 1992.

44. Cheng, Y.-B. and Thompson, D. P., Aluminium-containing nitrogen melilite phases. *J. Am. Ceram. Soc.*, 1994, **77**, 143–148.

45. Jama, S. A. B., Thompson, D. P. and Jack, K. H., The lithia–silicon nitride–alumina system. *Special Ceramics*, 1975, **6**, 299–308.